Letter of Intent for J-PARC: Intrinsic charm search at the J-PARC high momentum beamline

Y. Morino[1]*, K. Aoki[1], M. Naruki[2], K. Ozawa[1], and S. Yokkaichi[3]

[1] *KEK, High Energy Accelerator Research Organization, Tsukuba, Ibaraki 305-0801, Japan*
[2] *Department of Physics, Kyoto University, Sakyo-ku, Kyoto 606-8502, Japan*
[3] *RIKEN Nishina Center, RIKEN, Wako, Saitama 351-0198, Japan*

We propose a measurement of backward J/ψ production for 30 GeV protons incident on nuclear targets to search $|uudc\bar{c}\rangle$ Fock components in a proton (intrinsic charm). The existence of the intrinsic charm is expected to emerge as J/ψ suppression of the yield per nucleon at backward regions. The measurement can be carried out together with the J-PARC E16 experiment mainly. Moreover, an additional run of 60 shifts optimized for the J/ψ measurement is proposed. A model calculation and a GEANT4-based Monte-Carlo simulation are performed to evaluate a sensitivity of the measurement to the intrinsic charm. It is demonstrated that the proposed measurement has the good sensitivity for the intrinsic charm with probable magnitude.

1. Introduction

The existence of $|uudc\bar{c}\rangle$ Fock components in a proton, which is called *"intrinsic charm"*, was suggested in the early 1980's [1,2]. The intrinsic charm was introduced to account for the unexpected large cross section of charm in forward regions at first.

The intrinsic charm has two significant features as follows. The intrinsic charm tends to have a large momentum fraction (x), unlikely *"extrinsic charm"* which is generated by gluon splitting perturbatively. Second, parton distribution function (PDF) of the intrinsic charm can be different from the PDF of intrinsic anti-charm. These features of the intrinsic charm have been applied for possible solutions of various unexpected phenomena related with heavy quarks:*e.g.,* anomalous J/ψ suppression at large Feynman-x (x_F) regions in hadron-nucleus collisions [3–8], asymmetries between leading and non-leading charm hadro-production [9–13], anomalous large branching ratio of J/$\psi \to \rho\pi$ decay [14, 15], and hadro-production of double J/ψ at large x_F regions [16–19]. Since the intrinsic charm enables non-perturbative charm production, the cross section of charm will increase from the perturbative calculation especially at low energy regions. Therefore, this topic is closely related to the J-PARC E50 experiment and other possible experiments about heavy quarks at J-PARC. The intrinsic charm becomes an essential topic for not only hadron physics but also particle physics since the precise determination of PDF is crucial for the interpretation of measurements at Tevatron and LHC. It has been pointed out that the intrinsic charm is relevant to various interesting studies such as Higgs production, Z-boson production, single-top production, and dark matter searches [20–24]. Therefore, the confirmation and the quantitative evaluation of the intrinsic charm is a crucial baseline for the development of physics.

Despite a number of experimental and theoretical studies to evaluate a probability of the intrinsic

*Email: ymorino@post.kek.jp

charm in a proton (P_{IC}), even the existence of the intrinsic charm remains inconclusive. P_{IC} was initially suggested to be $\sim$ 1% [1]. $P_{IC} \sim 0.5\%$ was theoretically predicted by a chiral quark model [25]. Recently, P_{IC} was also calculated by lattice QCD, and their results were compatible with the result of the chiral quark model [26–28]. Experimentally, a straight and direct way to study the intrinsic charm is a measurement of the charm structure function from deep inelastic scattering. The charm structure function at large-x regions measured by EMC provided the positive result for the presence of the intrinsic charm [29]. P_{IC} evaluated from EMC data was $0.3 \sim 0.9\%$ depending on the used models [30–32]. The global analyses of the proton PDF with the intrinsic charm contribution were also carried out by several authors [33–36]. However, there is a significant tension between HERA [37] and EMC data in regions of overlapping kinematics. The results of the global analyses strongly depends on the choise of input data sets and the treatment of the tension: varing from $P_{IC} \leq\sim 0.2\%$ at the 5σ level to $P_{IC} \sim 4\%$. The current status of the P_{IC} analyses is reviewed in Ref. [38]. In summary, the existence of the intrinsic charm is neither rejected nor confirmed and P_{IC} seems to be less than a few % level even if it exists.

It is obvious that additional experimental results are necessary to the confirmation and the quantitative evaluation of the intrinsic charm. One of the solutions to this situation is to perform a precise measurement of the charm structure function at large-x regions, which could be carried out at the future electron-ion collider. Another way is an identification of a characteristic phenomenon of the intrinsic charm by a measurement of observables to be sensitive to the large-x charm component. Backward J/ψ production in low energy proton-nucleus collisions is a sensitive and clean observable to the existence of the intrinsic charm. The effect of the intrinsic charm will emerge as the J/ψ suppression of the yield per nucleon at backward regions. In this letter, we propose a new measurement to confirm the intrinsic charm by using a 30 GeV proton beam at the J-PARC high momentum beamline and the J-PARC E16 spectrometer [39]: A measurement of backward J/ψ production in proton-nucleus collisions. The new measurement can be carried out together with the E16 experiment, although an additional run of less than a month optimized for the J/ψ measurement is necessary.

The J/ψ suppression at large x_F in hadron-nucleus collisions is briefly reviewed, and then a basic idea in this study is explained in Sec. 2. Experimental setup is described in Sec. 3. Sec. 4 describes a model calculation to evaluate the effect of the intrinsic charm on the J/ψ suppression. Sec. 5 describes a Monte-Carlo detector simulation to evaluate reconstruction efficiency of J/ψ. The additional run (*"special run"*) is proposed in Sec. 6. An expected result is obtained in combination with Sec. 4-6, and then the result is discussed in Sec. 7. The summary of this letter is given in Sec. 8.

2. J/ψ suppression at large x_F in hadron-nucleus collisions

A number of experiments have reported the anomalous J/ψ suppression of the yield per nucleon at large x_F in hadron-nucleus collisions [3–7]. Figure 1(a) shows the dependence of the J/ψ cross section on a nuclear number (A) in terms of α as a function of x_F measured at E866, E772, and NA3 [3–5]. α is defined by $\sigma_A = \sigma_N \times A^\alpha$, where σ_N is the cross section on a nucleon. α is close to 1 at $x_F <\sim 0.3$, which indicates that J/ψ is produced by hard processes and interaction between J/ψ and the nuclear matter is not strong. It is consistent with the typical picture for a heavy quarkonium. However, α decreases to $\sim 2/3$ as x_F becomes larger, which means J/ψ production is strongly suppressed by the nuclear matter. When J/ψ is considered to be produced by the hard processes conventionally, this suppression pattern indicates only forward J/ψ strongly interacts the nuclear matter. These results are surprising since they contradict the picture of color transparency due to the smallness of heavy quarkonium and the x_F dependence of the J/ψ suppression also contradicts pQCD factorization [40]. On the other hand, Fig. 1(b) shows ratios of the dimuon yield from Drell-Yan process per nucleon for Fe/Be (Top) and W/Be (Bottom) as a function of x_F from E772 and E866 [41]. α for the Drell-Yan dumon is still ~ 0.95 at the most forward region. Therefore, the J/ψ suppression cannot be interrupted

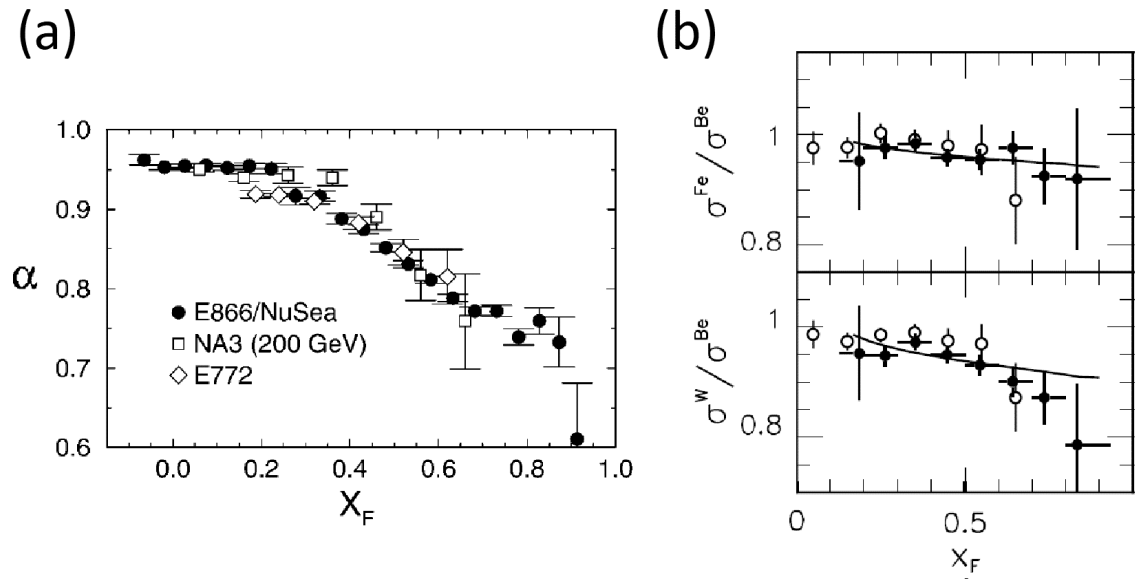

Fig. 1. (a): α for J/ψ as a function of x_F from E866 (solid circles), E772 (diamonds), and NA3 (open squares) [4]. α is defined by $\sigma_A = \sigma_N \times A^\alpha$. (b): Ratios of the dimuon yield from Drell-Yan process per nucleon for Fe/Be (Top) and W/Be (Bottom) as a function of x_F from E772 (open circles) and E866 (solid circles) [41].

as the result of nuclear shadowing and/or initial parton energy loss. Some specific effects for the heavy quarkonium must be considered. Two scenarios resolve this puzzle of the J/ψ suppression in hadron-nucleus collisions.

One of the solutions for the J/ψ suppression puzzle is an introduction of *"soft"* production of J/ψ due to the intrinsic charm [8, 42]. It assumes the following process. The intrinsic charm Fock state ($|uudc\bar{c}\rangle$) emerges in the incident proton ($|ud\bar{c}c\bar{c}\rangle$ in the case of the π^+ beam). The light quark components in the incident proton interact with soft gluons emitted from the nuclear surface. The remaining $c\bar{c}$ pair hadronizes to quarkonium and passes through the nucleus due to their smallness. This process is almost occurred on the nuclear surface, leading to an approximate $A^{2/3}$ dependence. Figure 2(a) shows a conceptual view of the above process. The intrinsic charm must carry a large fraction of the longitudinal momentum of the incident proton in order to minimize the off-shell component of the proton with the large mass of charm. Therefore, J/ψ generated via the soft process tends to have large x_F, while the yield of J/ψ generated via the hard processes decreases rapidly with x_F. It can explain the J/ψ suppression pattern, that is, the intrinsic charm contribution becomes dominant for J/ψ production, and then α approaches 2/3 as x_F increases.

The other solution for the J/ψ suppression puzzle is an energy loss model of J/ψ [43–45]. Fig. 2(c) shows a conceptual view of the energy loss model. The most important assumption in the model is that a $c\bar{c}$ pair is produced in a color octet state via the hard processes and then hadronizes to J/ψ after the hadronization time (τ_ψ) in the rest frame of the $c\bar{c}$ pair. The $c\bar{c}$ pair remains the color octet state and interacts strongly with the nuclear matter until it hadronizes. Since a path length of the color octet state is proportional to its $\beta\gamma$, the fast $c\bar{c}$ pair loses its energy significantly enough to explain the suppression pattern. The energy loss model almost reproduces the J/ψ suppression pattern of the past measurements [45]. Since it is difficult to reject the energy loss model from the experimental results to date, the present J/ψ suppression cannot be regarded as an evidence of the intrinsic charm. Indeed, there is also a possibility that the J/ψ suppression pattern is the result of the combination of the intrinsic charm and the energy loss.

The measurement of backward J/ψ production in low energy hadron-nucleus collisions is attrac-

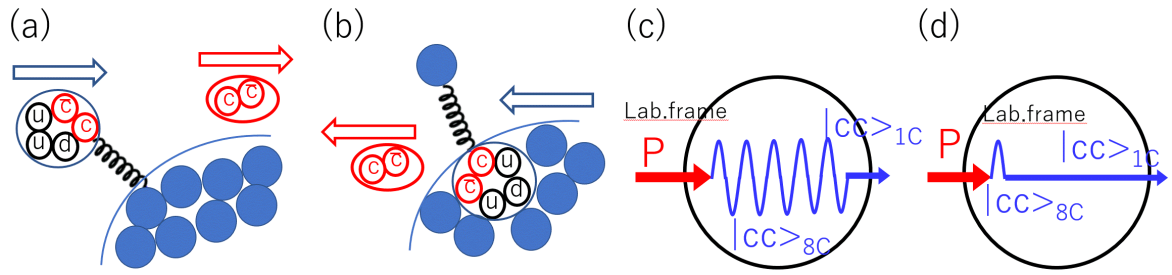

Fig. 2. Conceptual views of the two interpretation of the J/ψ suppression: (a) forward J/ψ production via the intrinsic charm, (b) backward J/ψ production via the intrinsic charm, (c) energy loss of the color octet in the case of forward production, and (d) energy loss of the color octet in the case of backward production.

tive to break through this situation. The energy loss of the $c\bar{c}$ color octet gets smaller in the case of backward production in low energy collisions, since the path length of the color octet becomes short due to its small β as shown in Fig. 2(d). On the other hand, the interaction between the intrinsic charm state ($|uudc\bar{c}\rangle$ or $|uddc\bar{c}\rangle$) emerged in the nucleon on the surface of the target and the incident proton produces backward J/ψ in a similar way to forward J/ψ production via the intrinsic charm (Fig. 2(b)). The contribution from the intrinsic charm is also expected to be almost independent of the collision energy [46]. When x_F of J/ψ gets close to -1 and the $c\bar{c}$ pair is sufficiently slow, the energy loss can be neglected while the effect of J/ψ production via the intrinsic charm will remain. Furthermore, the cross section of J/ψ via the hard processes gets considerably small in the case of low energy collisions. It leads that the fraction of the contribution from the intrinsic charm increases and backward J/ψ production gets to be more sensitive to the intrinsic charm. Therefore, the measurement of backward J/ψ production in low energy hadron-nucleus collisions is a powerful probe for the existence of the intrinsic charm. Such measurements have not been carried out yet. So far, the most backward measurement of J/ψ production ($x_F >\sim -0.3$) was carried out by HERA-B [6]. However, J/ψ production via the intrinsic charm is expected to appear at more backward regions and the $c\bar{c}$ pair is not sufficiently slow due to the high energy of the incident proton beam at HERA-B (920 GeV).

3. Experimental setup

Table I. Summary of the necessary conditions for the backward J/ψ measurement.

beam energy	beam intensity	targets	detectors
$>\sim$ 12 GeV	$>\sim 10^9$ ppp	several nuclei (light~heavy)	lepton spectrometer with backward acceptance and high rate tolerance

The measurement of backward J/ψ production in low energy hadron-nucleus collisions can be performed at the Hadron Experimental Facility at J-PARC. The measurement requires that an incident beam has enough energy to produce J/ψ and a beam intensity is high enough to compensate for the small cross section of J/ψ at low energy regions (nb order). The detectors for the measurement must have acceptance for backward J/ψ production, that is, a lepton spectrometer with large acceptance for backward scattering and high rate tolerance is suitable. Several experimental targets from light to heavy nuclei are necessary to measure the nuclear dependence of the J/ψ yield. The necessary conditions for the backward J/ψ measurement are summarized in Table. I.

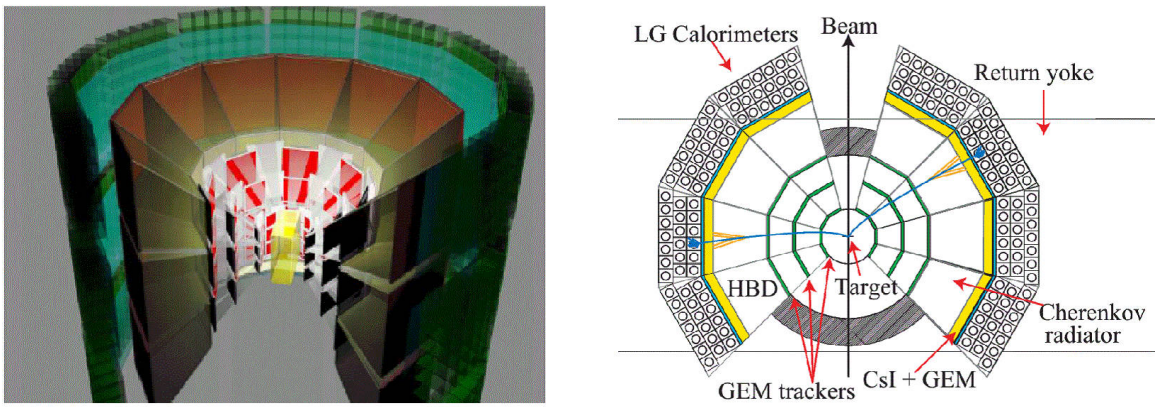

Fig. 3. The schematic view of the proposed E16 spectrometer: (Left) the 3D view and (right) the plan view.

The J-PARC E16 experiment already satisfies the requirements for the backward J/ψ measurement. The E16 experiment was proposed to perform a systematic study for the mass modification of light vector meson (ϕ and ω) by using the high-intensity proton beam at the J-PARC high momentum beamline with the new spectrometer [39]. The J-PARC high momentum beamline will deliver the 30 GeV proton beam with an intensity of 1×10^{10} protons per 2-second beam pulse in 5.52 second cycle. The schematic view of the proposed E16 spectrometer is shown in Figure 3. The E16 spectrometer is designed to have large acceptance for electrons from the slowly moving ϕ. The E16 spectrometer consists of 26 detector modules in the case of the full installation. The detectors are installed in a spectrometer magnet. The maximum field strength is 1.7 T at the center of the magnet, where nuclear targets are located. As the target, C, CH_2, Cu, and Pb are planned to be used for the systematic study of the nuclear dependence. The total thickness of the targets is planned to be less than ~2% radiation length to suppress the electron background originating from the γ conversion. The interaction length of the targets is less than ~0.5%. GEM Tracker (GTR) which has three tracking planes are located around the target to measure the momenta of charged particles [47]. Silicon Strip Detector (SSD) is also planned to be located at the innermost. Outside the tracker, Hadron Blind Detector (HBD) and lead-glass EM calorimeter (LG) are located successively to identify the electrons [48, 49].

A position resolution of 100 μm in the bending plane is required for the GTR, leading to mass resolution of 5 MeV/c^2 for the reconstructed ϕ. The GTR also cope with the high rate, 5 kHz/mm^2. In order to suppress the background originating from the electron miss-identification, the aimed miss-identification probability of the HBD and the LG are 1×10^{-2} and 4×10^{-2}, respectively.

A coincidental hit of a HBD segment and a LG block located just behind the segment is required with a corresponding hit on the most-outer GTR to trigger an electron track. Two electron candidates who have an opening angle of larger than a certain threshold ($40^\circ \sim 50^\circ$) are required for the trigger condition to select events including the slowly moving ϕ.

The data taking of backward J/ψ production will be performed together with the J-PARC E16 experiment basically. Furthermore, we propose an additional run of 60 shifts (20 days) to cope with the inefficiency of the normal E16 experiment for J/ψ at $x_F \sim 0$. It is called *"special run"* in this letter. The targets and the trigger condition will be optimized for the measurement of J/ψ at $x_F \sim 0$ during the special run. The detail of the special run is described in Sec. 6.

4. Model calculation of J/ψ yield

Estimation of the J/ψ suppression pattern in hadron-nucleus collisions is necessary to evaluate a quantitative sensitivity of the backward J/ψ measurement to search the intrinsic charm. The J/ψ yield in proton-nucleus collisions is also influenced by known nuclear effects, such as nuclear parton distribution and J/ψ absorption in nucleus, besides the intrinsic charm and the energy loss discussed in Sec. 2. A model calculation was performed to evaluate the sensitivity for the intrinsic charm in consideration of such nuclear effects. The model in this study considered the following processes and effects: the hard process and the soft process due to the intrinsic charm as the J/ψ production mechanisms, nuclear parton distribution function (nPDF) as the initial state effect, and the energy of the $c\bar{c}$ color octet and the J/ψ absorption in nucleus as the final state effects.

The J/ψ cross section via the hard process was evaluated by using leading order (LO) perturbative QCD (pQCD) and the color evaporation model (CEM) [50]. In the CEM, J/ψ production is treated identically to open charm production, except that the invariant mass of the $c\bar{c}$ pair is required to be less than the open charm threshold ($2m_D$ = 3.74GeV/c^2). Hence, the cross section of J/ψ is proportional to the integral value of the $c\bar{c}$ cross section over the pair mass from the $c\bar{c}$ production threshold ($2m_c$) to $2m_D$.

$$\frac{d\sigma_{\mathrm{J}/\psi}}{dx_F} = F_{\mathrm{J}/\psi} \int_{4m_c^2}^{4m_D^2} dm^2 \frac{d\sigma_{c\bar{c}}}{dx_F dm^2} \tag{1}$$

where, $F_{\mathrm{J}/\psi}$ is the fraction of the $c\bar{c}$ cross section leading to J/ψ production. In the CEM, $F_{\mathrm{J}/\psi}$ is a constant determined in comparison with the experimental results. The CEM has succeeded to reproduce many features of J/ψ production [51]. The cross section of the $c\bar{c}$ pair, $d\sigma_{c\bar{c}}/(dx_F dm^2)$, was calculated by the QCD factorization theorem and the LO pQCD (See Ref. [8,52] for details). According to Ref. [52], m_c was 1.5 GeV/c^2 and $F_{\mathrm{J}/\psi}$ was 0.17 in this study, respectively. The factorization and renormalization scale parameters were $2m_c$. We used CTEQ5L for the parton distribution of the nucleon [53]. Figure 4(a) shows the J/ψ cross section as a function of x_F calculated by the LO pQCD and the CEM in pp collisions at 30 GeV.

The J/ψ cross section via the soft process due to the intrinsic charm was evaluated similarly as Ref. [8,54]. The probability distribution of the intrinsic charm state ($|uudc\bar{c}\rangle$ or $|uddc\bar{c}\rangle$) in a nucleon was assumed as follows [1,2].

$$\frac{dP_{IC}}{dx_1 \cdot \cdot dx_5} = N_5 \frac{\delta\left(1 - \sum_{i=1}^{5} x_i\right)}{\left(m_p^2 - \sum_{i=1}^{5} (\hat{m}_i^2/x_i)\right)^2} \tag{2}$$

where, N_5 is a normalization factor for P_{IC} and $\hat{m}_i$ is an average traverse mass ($\sqrt{m_i^2 + < k_T^2 >}$). We assumed $\hat{m}$ of the light quark was 0.45 GeV/c^2 and $\hat{m}$ of the charm quark was 2.25 GeV/c^2 respectively since m_c = 1.5 GeV/c^2 was used in pQCD and $< k_T^2 > \propto m_i^2$ was expected. N_5 was left as the free parameter to adjust P_{IC}. The cross section of charm production via the intrinsic charm ($\sigma_{c\bar{c}}^{IC}$) is related to P_{IC} and the inelastic cross section (σ^{inel}) as follows.

$$\sigma_{c\bar{c}}^{IC} = P_{IC} \sigma^{inel} \frac{\mu^2}{4\hat{m}_c^2} \tag{3}$$

where, $\mu^2/4\hat{m}_c^2$ is the soft interaction factor to break the intrinsic charm state. μ^2 = 0.1 GeV^2 was used according to Ref. [8]. (it was determined in comparison with the J/ψ cross section measured at NA3.) The J/ψ cross section ($\sigma_{\mathrm{J}/\psi}^{IC}$) is related to the $c\bar{c}$ cross section via the intrinsic charm as in the CEM. Hence,

$$\frac{d\sigma_{\mathrm{J}/\psi}^{IC}}{dx_F} = F_{\mathrm{J}/\psi}^{IC} \sigma^{inel} \frac{\mu^2}{4\hat{m}_c^2} \int \prod_{i=1}^{5} dx_i \int_{4m_c^2}^{4m_D^2} dm^2 \frac{dP_{IC}}{dx_1 \cdot \cdot dx_5 dm^2} \delta(x_F - x_c - x_{\bar{c}}) \tag{4}$$

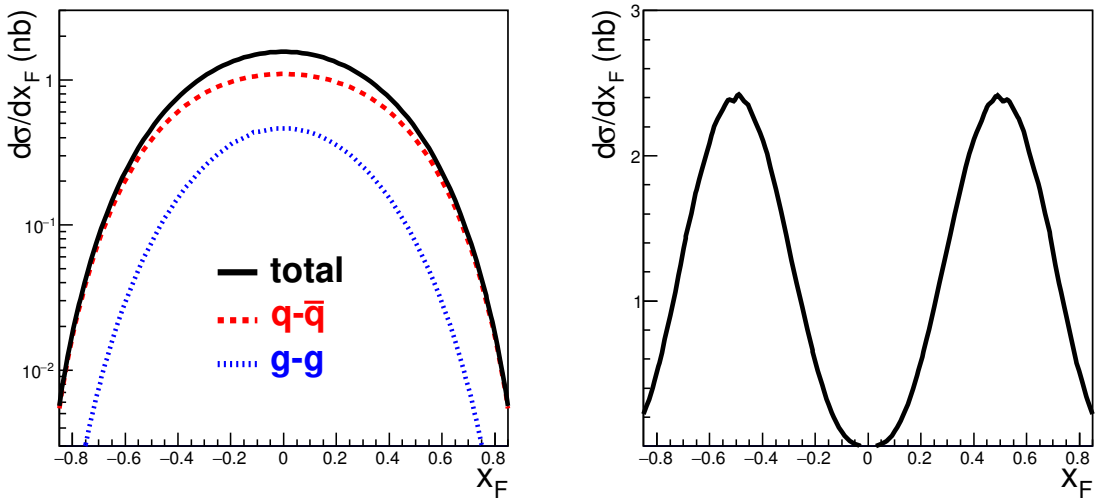

Fig. 4. The calculated J/ψ cross section as a function of x_F in pp collisions at 30 GeV. (Left) the hard process calculated by the LO pQCD and the CEM (red dashed line:$q - \bar{q}$ contribution, blue dotted line:$g - g$ contribution, black solid line:total yield). (Right) the soft process originating from the intrinsic charm in the case of $P_{IC} = 0.2\%$.

where, $F^{IC}_{J/\psi}$ is the fraction of the $c\bar{c}$ cross section via the intrinsic charm leading to J/ψ production. $F^{IC}_{J/\psi} = 0.17 \times 1/4$ was used, where 0.17 was common with the hard process and $1/4$ was *"the flavor suppression factor"* relating with the intrinsic charm process [54]. Gauss distribution was assumed for k_T in this integral. Fig. 4(b) shows the calculated J/ψ cross section via the soft process as a function of x_F in pp collisions at 30 GeV in the case of $P_{IC} = 0.2\%$. It is confirmed that the contribution from the soft process is concentrated at the large $|x_F|$ region. The nuclear dependence of this soft process is $A^{2/3}$.

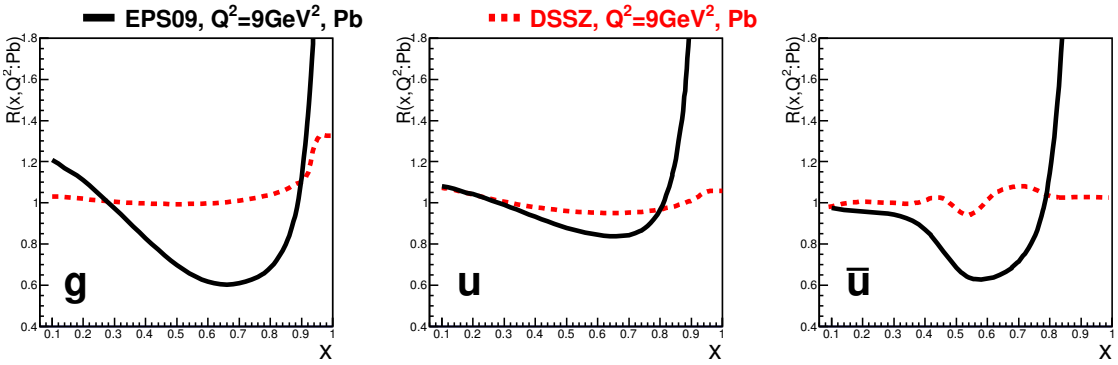

Fig. 5. The DSSZ and EPS09 nuclear effects to bound-proton PDFs in Pb as a function of x at the initial scales $Q^2 = 9\text{GeV}^2$ for gluon (left), u quark (middle), and $\bar{u}$ quark (right). Black solid lines represent the EPS09 and red dashed lines represent the DSSZ, respectively.

We used two results of the latest nPDF global analyses, called "EPS09" [55] and "DSSZ" [56], as nPDFs in this model calculation. Figure 5 shows the DSSZ and EPS09 nuclear effects to bound-

proton PDFs in Pb as a function of x at the initial scales $Q^2 = 9\text{GeV}^2$. Although there is not a major difference between DSSZ and EPS09 for the input experimental results as constraints for nPDFs, these two nPDFs differ at EMC region as shown at Fig. 5. The essential difference between the two analyses is that the DSSZ analysis uses the nuclear fragmentation functions [56]. The two analyses were used, and the results were compared to consider the uncertainty of nPDFs.

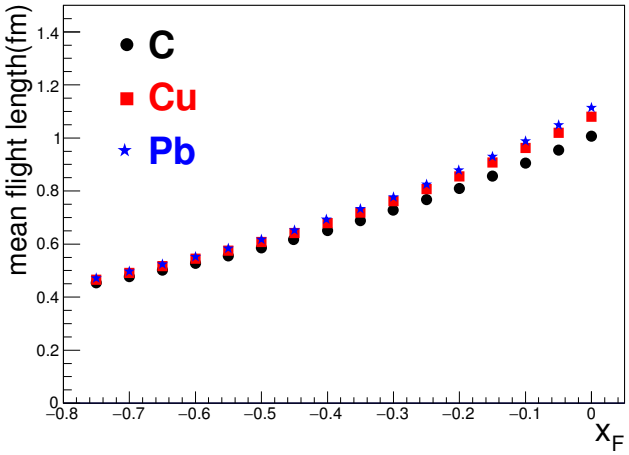

Fig. 6. The mean path length of the $c\bar{c}$ color octet in the nuclear matter as a function of x_F when the targets are C (black circles), Cu (red squares), and Pb (blue stars).

The path length of the $c\bar{c}$ color octet in the nuclear matter was calculated assuming $\tau_\psi = 0.3$ fm, which was evaluated based on the uncertainty principle [43]. The $c\bar{c}$ color octet was produced uniformly in the nucleus, and then the path length in the nuclear matter was calculated as a function of x_F. Figure 6 shows the mean path length of the color octet as a function of x_F in the case when the targets are C, Cu, and Pb. Most of the color octet change to the color singlet in the nuclear matter even if the target is C. Therefore, the mean fight length of the color octet is almost the same from C to Pb, leading that the energy loss is also the same from C to Pb. The energy loss of the color octet consequently does not make the nuclear dependence if C is used as the reference. In the above reason, the energy loss of the color octet was neglected in this model calculation.

The path length of J/ψ in the nuclear matter was calculated similarly as the $c\bar{c}$ color octet. Then, the survival probability of J/ψ in nucleus was calculated according to $\exp(-L_\psi \rho \sigma_{abs})$, where L_ψ is the path length of J/ψ in the nuclear matter, ρ (0.17 fm^{-3}) is the nuclear density, and σ_{abs} is the J/ψ absorption cross section, respectively. $\sigma_{abs} = 10$ mb was assumed in this study based on extrapolation of various results summarized in Ref. [57]. Although this assumption is determined by rough extrapolation, the uncertainty of this parameter does not change much the shape of the J/ψ suppression pattern.

The J/ψ suppression pattern was evaluated based on the above processes for 30 GeV protons incident on the nucleus. Figure 7 shows the evaluated J/ψ suppression degree in terms of α as a function of x_F. The left panel shows the result in the case of nPDF=EPS09 and the right panel shows one in the case of nPDF=DSSZ, respectively. P_{IC} is varied from 0% to 1.0% in Fig. 7. While α at $x_F \sim 0$ does not depend on P_{IC}, α at large negative x_F degrees clearly depending on P_{IC} in both nPDF. The deviation of α at $x_F \sim 0$ from 1 is the result of the J/ψ nuclear absorption and nPDF. The effect of the intrinsic charm appears as the deviation of α at large negative x_F from α at $x_F \sim 0$. While $P_{IC} < 0.2\%$ at the 5σ level is the most negative result of the current study, the effect of the intrinsic

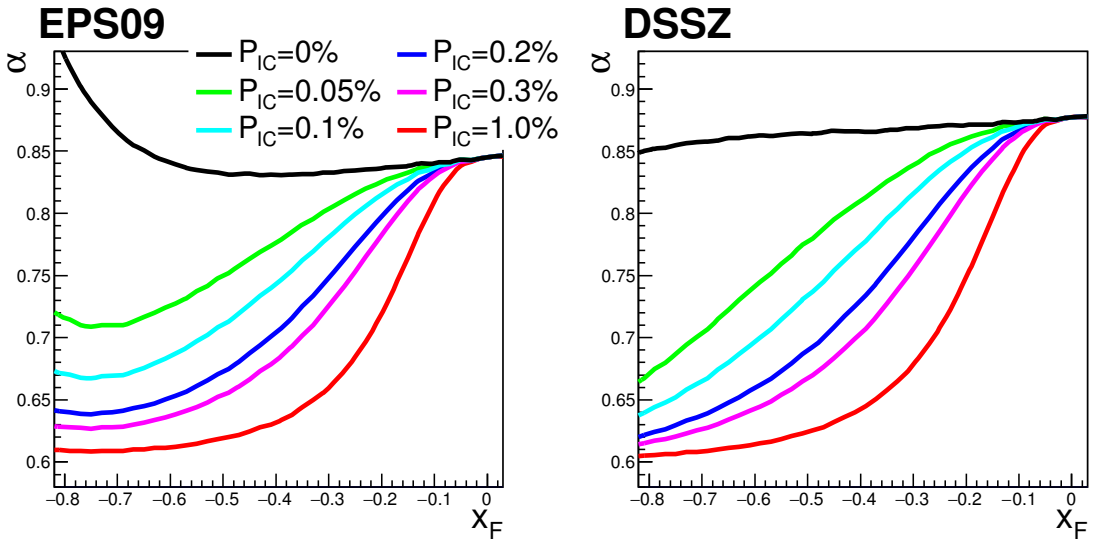

Fig. 7. The evaluated J/ψ suppression degree (α) as a function of x_F with various P_{IC} in the case of nPDF=EPS09 (left) and nPDF=DSSZ (right).

charm can be clearly seen at Fig. 7 even in the case of $P_{IC} = 0.05\%$. The sensitivity of backward J/ψ production at 30 GeV to the intrinsic charm is fairly well.

5. Simulation analysis

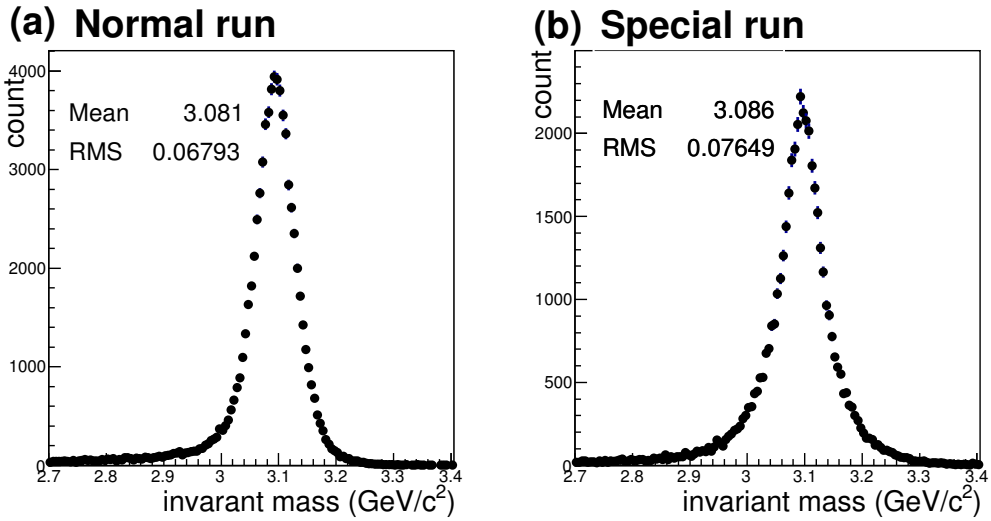

Fig. 8. The simulated invariant mass distributions for the reconstructed J/ψ: (a) the normal run and (b) the special run.

A full detector Monte-Carlo simulation based on GEANT4 packages was performed to evaluate the reconstruction efficiency of J/ψ and the trigger rate from backgrounds [58]. The full installation

of 26 modules was assumed for the E16 spectrometer. The detector response in the simulation was roughly tuned based on the achieved detector performance in test experiments. The data taking of backward J/ψ production is assumed to be performed together with the J-PARC E16 experiment in this section. It is called *"normal run"* in this letter.

400 μm C, 80 μm Cu and 20 μm Pb are planned to be used as the targets of the E16 experiment. The trigger condition is the same as the E16 experiment. An electron track candidate at the trigger level requires a coincidental hit of a HBD segment, a LG block located just behind the segment, and a corresponding most-outer GTR segment. Although planned thresholds for hit decision of the HBD and the LG were not determined precisely, (number of photo-electron)≥4 was required for the HBD hit and (energy deposit at the LG block) ≥0.4 GeV was required for the LG hit in this simulation, respectively.

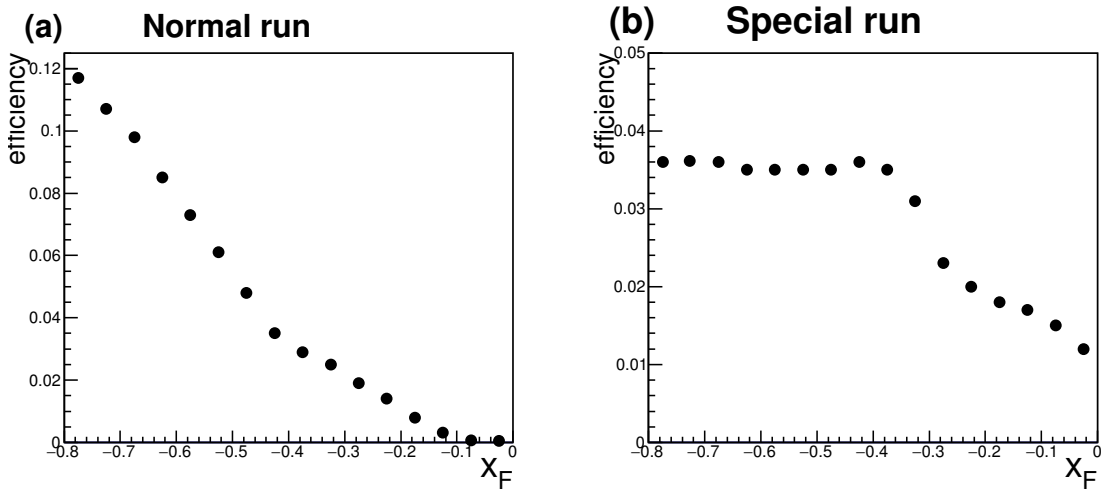

Fig. 9. The evaluated reconstruction efficiency of J/ψ as a function of x_F: (a) the normal run and (b) the special run.

A large opening angle between two electron track candidates is also required for the trigger condition. The opening angle is determined by the distance between the two fired HBD trigger segments of the candidate pair. To determine the threshold of the opening angle, background events from the vacuum film and the targets were generated by nuclear cascade code JAM [59], and the secondary interaction in materials were simulated by the full detector simulation. When (direct distance)>7 segments and (vertical distance)≥1 segments were required for the two HBD segments of the candidate pair, the trigger rate was reduced to less than 1 kHz which was possible to deal with the E16 read-out system. Therefore, the above condition was used as the trigger condition in this study.

The reconstruction efficiency of J/ψ was studied by using the full detector simulation. Events which only include a decay electron pair from J/ψ with various momentum are simulated. An offline analysis was performed for the events satisfy the above trigger condition. Electron tracks were reconstructed using hit information of the SSD and the GTR. Associated hits at the HBD and the LG with the reconstructed track were required to identify electrons. The HBD hit corresponding to the track with (number of photo-electron)≥4 was required for each track. The energy deposit at the LG was defined as the sum of the energy deposit at 5 LG blocks which were the LG block corresponding to the track and the four quarters of it. (energy deposit)>0.9 GeV or (energy deposit)/(momentum)>0.3 were also required for each track. Since this simulation study was performed to evaluate the feasibility of the measurement, the analysis cut was somewhat loose. Figure 8(a) shows the simulated invari-

ant mass distributions for the reconstructed J/ψ in the case of the normal run. Figure 9(a) shows the evaluated reconstruction efficiency of J/ψ as a function of x_F for the normal run. The reconstruction efficiency in Fig. 9(a) includes the geometrical acceptance, the efficiency of the track reconstruction, the efficiency of the electron identification and the trigger efficiency. Although the efficiency is quite well at large negative x_F, most of J/ψ at $x_F > -0.2$ cannot be reconstructed.

6. Proposed special run

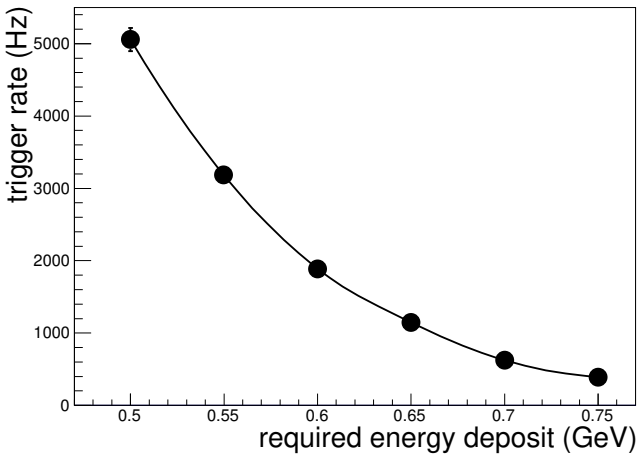

Fig. 10. The evaluated trigger rate as a function of the required energy deposit at the LG block in the case of the special run.

The special run is proposed to cope with the inefficiency for J/ψ at $x_F \sim 0$ as shown in Fig. 9(a). The targets are moved upstream by 23 cm near a vacuum film of a beam pipe. Data taking with 60 shifts (20 days) for the special run is necessary to collect enough statistics. The targets and the trigger condition will be optimized for the measurement of J/ψ at $x_F \sim 0$ during the special run. 800 μm C and 400 μ Pb were selected in this study. Since the heavy nucleus was advantageous to study the nuclear dependence, the thick Pb target was selected. The total interaction length of the targets is ~0.4%, which is the almost same as the normal run. The E16 spectrometer is enable to deal with the expected event rate. On the other hand, the total radiation length is ~7.5%. It is about 5 times as thick as the total radiation length of the normal targets due to the thick Pb target, leading to increase of backgrounds from the γ conversion.

The trigger must be optimized to handle the increased backgrounds from the γ conversion, while the backgrounds do not matter at the offline analysis since the J/ψ peak is far from the contribution from the γ conversion. The trigger optimization was performed by using the full Monte-Carlo simulation and the JAM code. Since electrons from J/ψ at $x_F \sim 0$ have significantly higher energy than the background electrons, the requirement of a high energy deposit at the LG block for the trigger is effective to suppress the trigger rate without reducing the efficiency. The relation between the expected trigger rate and the threshold energy at the LG was studied in the similar way to the normal run. The coincidence condition was optimized for the upstream targets and the required opening angle was changed to be (direct distance)≥7 HBD segments. Figure 10 shows the evaluated trigger rate as a function of the threshold for the LG hit. As shown in Fig. 10, the threshold of 0.7 GeV is enough to reduce the trigger rate to less than 1 kHz. This trigger condition satisfy the requirement of the E16

read-out system.

The offline analysis was also performed similarly as the normal run. The threshold for the LG hit was assumed to be 0.7 GeV. Figure 8(b) shows the simulated invariant mass distributions for the reconstructed J/ψ in the case of the special run. Figure 9(b) shows the evaluated reconstruction efficiency of J/ψ as a function of x_F for the special run. The reconstruction efficiency in the special run is higher than one in the normal run at $x_F > -0.3$. J/ψ at $x_F \sim 0$ can be reconstructed although the efficiency is not very well.

7. Expected experimental result

Table II. Summary of the parameters used to normalize the statistics.

	beam intensity	shifts	targets	pair reconstruction efficiency	S/B
normal run	10^{10} ppp	300 (100 days)	400 μm C, 100 μm Ti, 80 μm Cu, 20 μm Pb	43%	5/1
special run	10^{10} ppp	60 (20 days)	800 μm C, 100 μm Ti, 400 μm Pb	43%	5/1

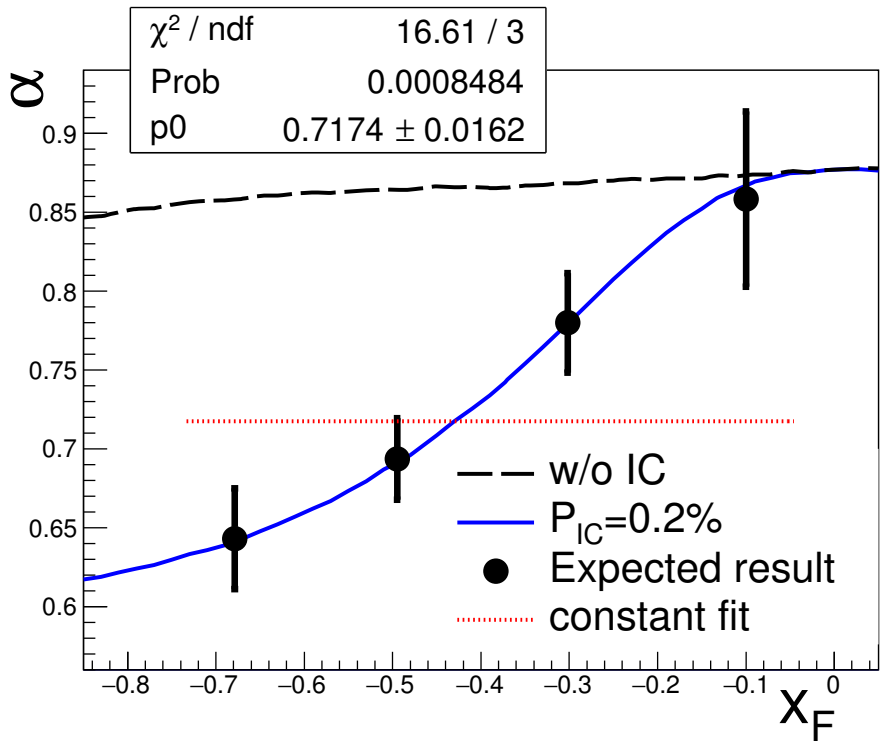

Fig. 11. The expected experimental result (black circles) in t he case of nPDF=DSSZ and $P_{IC} = 0.2\%$, and the model calculations without IC (black dashed line) and with $P_{IC} = 0.2\%$ (blue smooth line). The red dotted line shows the constant fit result.

An expected J/ψ yields were evaluated by using the J/ψ cross section in Fig. 4, the J/ψ suppression degree in Fig. 7, and the reconstruction efficiency in Fig. 9. A pair reconstruction efficiency, which was the efficiency originating from the track finding and fitting under background hits with 5 kHz/mm^2, was also included in the normalization. The pair reconstruction efficiency was assumed to be 43%, which was studied at the ϕ yield estimation of the E16 experiment [60]. The efficiency for DAQ live time was not considered in this letter. The Ti vacuum film was also treated as the nuclear target, hence, the statistics of J/ψ from the vacuum film were considered. The signal to background ratio of the J/ψ yield was assumed to be 5/1. The statistics were normalized to the 300 shifts (100 days) for the normal run and the 60 shifts (20 days) for the special run, respectively. The parameters used to normalize the statistics are summarized in Table. II.

Figure 11 shows the expected experimental result in the case of nPDF=DSSZ and $P_{IC} = 0.2\%$. In the figure, the blue smooth line shows the model calculation with $P_{IC} = 0.2\%$ and the black dashed line shows one without the intrinsic charm. When the expected result is compared with the calculation without the intrinsic charm, χ^2/ndf is 96.8/4. The model without the intrinsic charm can be rejected with the expected experimental uncertainty. A constant value fit was also applied to the expected result. It corresponds to that the α curve without the intrinsic charm is approximated by a constant value, and an absolute value of the constant is optimized by changing σ_{abs}. The red dotted line in Fig. 11 shows the constant fit result, where the resulting α is $\sim$ 0.72 corresponding $\sigma_{abs} \sim$ 37 mb. Even though $\sigma_{abs} \sim$ 37 mb is obviously too large than the possible value, χ^2/ndf of the fit is still 16.6/3, leading to the rejection of the fit with $\sim$ 99.92% probability. The measurement of backward J/ψ production will reveal the effect of the intrinsic charm in this case as described above.

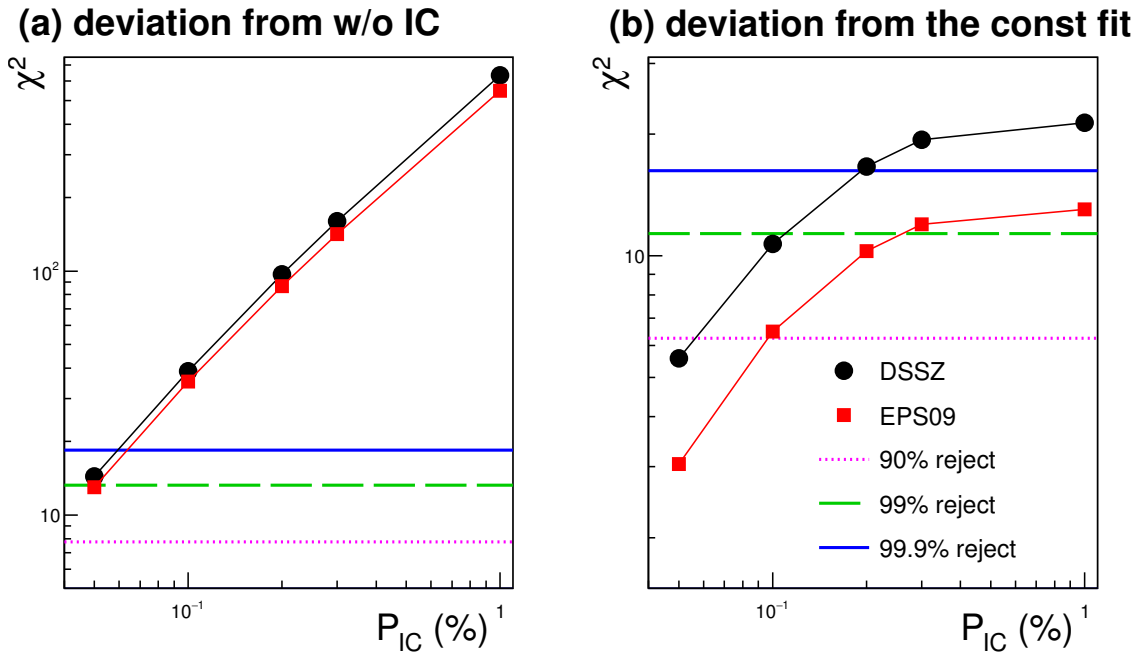

Fig. 12. The evaluated χ^2 as a function of P_{IC}: (a) χ^2 of the comparison between the expected results and the calculation without the intrinsic charm and (b) χ^2 of the constant fit. The black circles show the results with nPDF=DSSZ and the red squares show the results with nPDF=EPS09, respectively. The straight lines represent χ^2 corresponding various rejection level (blue smooth lines:99.9% rejection, green dashed lines:99% rejection, magenta dotted lines:90% rejection).

The sensitivity to the effect of the intrinsic charm was evaluated by the above two methods in a variety of P_{IC} and nPDFs, although the evaluation method of the sensitivity is still open to argument. Figure 12 shows the evaluated χ^2 as a function of P_{IC}. Fig. 12(a) shows χ^2 of the comparison between the expected results and the model calculation without the intrinsic charm and Fig. 12(b) shows χ^2 of the constant fit, respectively. In this figure, the black circles show the results with nPDF=DSSZ and the red squares show the results with nPDF=EPS09, respectively. When σ_{abs} is fixed to be 10 mb, which is the probable value, the sensitivity to the intrinsic charm is quite well even for $P_{IC} \sim 0.05\%$ level as shown in Fig. 12(a). Even if σ_{abs} is changed freely, the measurement has the sensitivity to the intrinsic charm for $P_{IC} = 0.1 \sim 0.2\%$ level as shown in Fig. 12(b). When the probable range of σ_{abs} is considered, the sensitivity will be improved. Since P_{IC} seems to be less than a few % level and the theoretical prediction is $P_{IC} \sim 0.5\%$, the enough sensitivity is demonstrated for the interested region. In conclusion, the E16 experiment with the special run of 60 shifts will provide the crucial data for the existence of the intrinsic charm.

8. Summary

The intrinsic charm is a long-standing problem. The existence of the intrinsic charm remains inconclusive, although a number of experimental and theoretical studies have been performed to reveal it.

The past measurements of J/ψ production have found the anomalous J/ψ suppression at large x_F in hadron-nucleus collisions, which is considered to be relevant with the intrinsic charm. However, the J/ψ suppression has not been regarded as the evidence of the intrinsic charm due to the similar result from the possible large energy loss of the $c\bar{c}$ color octet.

The measurement of backward J/ψ production in proton-nucleus collisions was proposed in this letter by using the proton beam at the J-PARC high momentum beamline and the J-PARC E16 spectrometer. The observation of the J/ψ suppression in the proposed measurement will be the crucial evidence since the effect of the energy loss of the $c\bar{c}$ color octet is expected to disappear due to its short path length in the nucleus.

The model calculation was performed to evaluate the cross section of J/ψ production and the suppression pattern in proton-nucleus collisions. The model considered the hard process and the soft process due to the intrinsic charm as the J/ψ production mechanisms. Nuclear parton distribution function and the J/ψ absorption in the nucleus were also considered as the known nuclear effects. The energy loss of the $c\bar{c}$ color octet was neglected since it was turned out that the effect was canceled out.

The reconstruction efficiency of J/ψ was evaluated by using the GEANT4-based Monte-Carlo simulation. The trigger rate from the backgrounds was also evaluated by the detector simulation and the nuclear cascade code. The special run of 60 shifts was proposed to cope with the inefficiency for J/ψ at $x_F \sim 0$ in the case of the normal E16 experiment.

The statistics of the expected results were evaluated based on the cross section of J/ψ, the reconstruction efficiency, and the reasonable assumption of the run condition. The sensitivity to the intrinsic charm was discussed with the expected uncertainty of the experiment. It was confirmed that the measurement of backward J/ψ production at the E16 experiment with the special run had the good sensitivity for the intrinsic charm with a probable value of P_{IC}.

References

[1] S. J. Brodsky, P. Hoyer, C. Peterson, and N. Skai, Phys. Lett. **B 93** 451 (1980).
[2] S. J. Brodsky, C. Peterson, and N. Skai, Phys. Rev. D **23** 2745 (1981).
[3] J. Badier *et al.*, Z. Phys. **C20** 101 (1983).
[4] M. J. Leitch *et al.*, Phys. Rev. Lett **84** 3256 (2000).
[5] D. M. Alde *et al.*, Phys. Rev. Lett **66** 133 (1991).

[6] I. Abt *et al.*, Eur. Phys. J. **C60** 525 (2009).
[7] R. Arnaldi *et al.*, Phys. Lett. **B706** 263 (2012).
[8] R. Vogt, Phys. Rev. C **61** 035203 (2000).
[9] E. M. Aitala *et al.*, Phys. Lett. **B371** 157 (1996).
[10] P. Chauvat *et al.*, Phys. Lett. **B199** 304 (1987).
[11] M. I. Adamovich, *et al.*, Eur. Phys. J.**C8** 593 (1999).
[12] F. G. Garcia *et al.*, Phys. Lett. **B528** 49 (2002).
[13] T. Gutierrez and R. Vogt, Nucl. Phys. **B539** 189 (1999).
[14] Particle Data Group. Chin. Phys. C **40**, 100001 (2016).
[15] S. J. Brodsky and M. Karliner, Phys. Rev. Lett **78** 4682 (1997).
[16] M. Mattson *et al.*, Phys. Rev. Lett. **89** 112001 (2002).
[17] J. Badier *et al.*, Phys. Lett. **B158** 457 (1985).
[18] R. Vogt and S. J. Brodsky, Phys. Lett. **B349** 569 (1995).
[19] S. Koshkarev and V. Anikeev, Phys. Lett. **B765** 171 (2017).
[20] S. J. Brodsky, B. Kopeliovich, I. Schmidt, and J. Soffer, Phys. Rev. D **73** 113005 (2006).
[21] T. Boettcher, P. Ilten, and M. Williams, Phys. Rev. D **93** 074008 (2016).
[22] J. Pumplin, H. L. Lai and W. K. Tung, Phys. Rev. D **75** 054029 (2007).
[23] J. R. Ellis, K. A. Olive, and C. Savage, Phys. Rev. D **77** 065026 (2008).
[24] J. Giedt, A. W. Thomas, and R. D. Young, Phys. Rev. Lett **103** 201802 (2009).
[25] T. Hatsuda and T. Kunihiro, Nucl. Phys. **B387** 715 (1992).
[26] A. Abdel-Rehim *et al.*, Phys. Rev. Lett **116** 252001 (2016).
[27] W. Freeman and D. Toussaint, Phys. Rev. D **88** 054503 (2013).
[28] M. Gong *et al.*, Phys. Rev. D **88** 014503 (2013).
[29] J. J. Aubert *et al.*, Nucl. Phys. **B213** 31 (1983).
[30] E. Hoofmann and R. Moore, Z. Phys. **C20** 71 (1983).
[31] B. Harris, J. Smith, and R. Vogt, Nucl. Phys.**B461** 181 (1996).
[32] F. M. Steffens, W. Melnitchouk, and A. W. Thomas, Eur. Phys. J.**C11** 673 (1999).
[33] J. Pumplin, H. L. Lai, and W. K. Tung, Phys. Rev. D **75** 054029 (2007).
[34] P. M. Nadolsky *et al.* , Phys. Rev. D **78** 012004 (2008).
[35] S. Dulat *et al.* , Phys. Rev. D **89** 073004 (2014).
[36] P. Jimenez-Delgado, T. J. Hobbs, J. T. Londergan, and W. Melnitchouk, Phys. Rev. Lett **114** 082002 (2015).
[37] H. Abramowicz *et al.*, Eur. Phys. J.**C73** 2311 (2013).
[38] S. J. Brodsky *et al.*, Adv. High Energy Phys.**2015** 231547 (2015).
[39] S. Yokkaichi, Lect. Notes. Phys.**C781** 161 (2009).
[40] P. Hoyer, M. Vanttinen and U. Sukhatme, Phys. Lett. **B246** 217 (1990).
[41] M. A. Vasiliev *et al.*, Phys. Rev. Lett **83** 2304 (1999).
[42] S. J. Brodsky and P. Hoyer, Phys. Rev. Lett **63** 1566 (1989).
[43] D. Kharzeev and H. Satz, Z. Phys. **C60** 389 (1993).
[44] F. Arleo, P. B. Gossiaux, T. Gousset, and J. Aichelin, Phys. Rev. C **61** 054906 (2000).
[45] F. Arleo and S. Peigné, Phys. Rev. Lett **109** 122301 (2012).
[46] R. Vogt, S. J. Brodsky and P. Hoyer, Nucl. Phys. **B360** 67 (1991).
[47] Y. Komatsu *et al.*, Nucl. Instrum. Meth. A **732** 241 (2013).
[48] K. Aoki *et al.*, Nucl. Instrum. Meth. A **628** 300 (2011).
[49] K. Kanno *et al.*, Nucl. Instrum. Meth. A **819** 20 (2016).
[50] H. Fritzsch, Phys. Lett. **B67** 217 (1977).
[51] G. A. Schuler and R. Vogt, Phys. Lett. **B387** 181 (1996).
[52] J. C. Peng, D. M. Jansen and Y. C. Chen, Phys. Lett. **B344** 1 (1995).
[53] H. L. Lai *et al.*, Eur. Phys. J. **C12** 375 (2000).
[54] R. Vogt and S. J. Brodsky, Phys. Lett. **B349** 569 (1995).
[55] E. J. Eskola, H. Paukkunen and C. A. Salgado, J. High. Energy. Phys **04** 065 (2009).
[56] D. de Florian, R. Sassot, P. Zurita and M. Stratmann, Phys. Rev. D **85** 074028 (2012).
[57] C. Lourenco, R. Vogt and H. K. Woehri, J. High. Energy. Phys **02** 014 (2009).
[58] S. Agostinelli *et al.*, Nucl. Instrum. Meth. A **506** 250 (2003).
[59] Y. Nara *et al.*, Phys. Rev. C **61** 024901 (2000).
[60] S. Yokkaichi *et al.*, J-PARC E16 Run0 proposal
https://j-parc.jp/researcher/Hadron/en/pac_1707/pdf/E16_2017-10.pdf